Regioselective Hydroacylation

DOI: 10.1002/anie.201100956

Rhodium-Catalyzed Branched-Selective Alkyne Hydroacylation: A Ligand-Controlled Regioselectivity Switch**

Carlos González-Rodríguez, Rebekah J. Pawley, Adrian B. Chaplin, Amber L. Thompson, Andrew S. Weller, and Michael C. Willis**

With the identification of new catalysts[1] and the development of strategies such as chelation control,[2] transition metal-catalyzed intermolecular alkene and alkyne hydroacylation reactions are becoming useful methods for the preparation of ketones.[3] Although substrate limitations still exist, the current methods allow the preparation of a broad range of functionalized products. Consequently, it is perhaps not surprising that several recent reports have begun to address the control of reaction selectivity. In particular, a number of enantioselective processes have recently been described.[4] Control of regioselectivity in hydroacylation reactions has also been explored, but usually with the caveat that a particular set of reaction substrates lead to a fixed regiochemical outcome. Linear selectivity represents the most common reaction pathway for both alkene and alkyne hydroacylation reactions, and although several branched-selective reactions are known, they usually require a specific combination of substrates. For example, provided that aromatic aldehydes and terminal alkyl alkynes are employed, Jun et al. have utilized a Rh/picoline cocatalytic system to report a highly branched-selective alkyne process;[5] Krische et al.[1d] and Ryu et al.[1c] have both reported branched-selective Ru-catalyzed diene hydroacylations; Suemune et al.[2a,4d] and Dong et al.[4g] have exploited chelating alkenes to achieve branched-selectivity, and Krische et al. have described a branched-selective reductive hydroacylation protocol employing styryl substrates.[1a] The ability to selectively access branched products from alkene hydroacylation presents opportunities for asymmetric synthesis,[4d,g] while the alkyne adducts are synthetically useful *exo*-methylene enones. However, as far as we are aware, there are no examples of catalyst or ligand control being used to switch between linear and branched products for a given substrate combination (Scheme 1).[6]

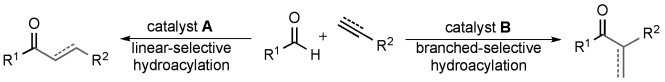

Scheme 1. Catalyst-controlled linear- and branched-selective alkene and alkyne hydroacylation reactions.

During our studies on the use of β-*S*-substituted aldehydes in chelation-controlled intermolecular alkene and alkyne hydroacylation reactions we have observed almost complete selectivity for the linear adducts.[7,8] However, in the context of exploring an asymmetric process we observed that when a DIPAMP-derived Rh-catalyst was employed for the combination of aldehyde **1a** and phenylacetylene (**2a**) the ketones (**3a** + **4a**) were obtained as a 1:4 mixture of branched and linear regioisomers (Table 1, entry 1). This is in contrast with the use of the parent dppe-derived catalyst, which delivers the same products in a 1:10 branched:linear ratio (Table 1, entry 2). Intrigued by this observation we now report the use of related *ortho*-substituted dppe-derived ligands, **5**, in the development of branched-selective alkyne hydroacylation reactions. These ligands have previously been employed in alkene/CO copolymerization chemistry, where structure–activity relationships have been outlined.[9]

Table 1: Ligand effects on the Rh-catalyzed hydroacylation reaction of aldehyde **1a** and phenylacetylene.[a]

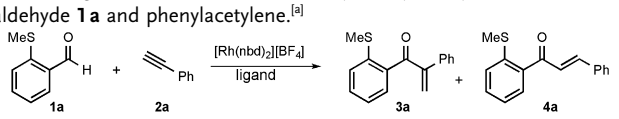

Entry	Ligand (R)	Conversion [%][b]	**3a**:**4a**[b]
1	DIPAMP	100	1:4
2	dppe	100	1:10
3	**5a** (*o*-Me)	100	1:2.5
4	**5b** (*o*-Et)	100	1:1
5	**5c** (*o*-*i*Pr)	100[c]	3:1
6	**5d** (*o*-Cy)	100	2.5:1
7	**5e** (*o*-*t*Bu)	45	1:3
8	**5f** (*p*-*i*Pr)	100	1:7

[a] Conditions: aldehyde (0.3 mmol), alkyne (0.45 mmol), $[Rh(nbd)_2][BF_4]$ (10 mol%), ligand (10 mol%), acetone (2 mL), 50°C, 12 h. nbd = norbornadiene. [b] Determined by ^{1}H NMR analysis of the crude reaction mixtures. [c] 79% yield of isolated product.

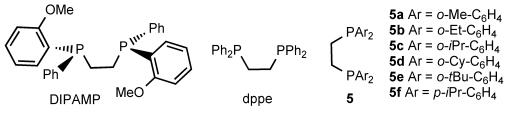

[*] Dr. C. González-Rodríguez, R. J. Pawley, Dr. A. B. Chaplin, Dr. A. L. Thompson, Prof. A. S. Weller, Dr. M. C. Willis
Department of Chemistry, University of Oxford
Chemistry Research Laboratory
Mansfield Road, Oxford, OX1 3TA (UK)
Fax: (+44) 1865-28-5002
E-mail: michael.willis@chem.ox.ac.uk
Homepage: http://mcwillis.chem.ox.ac.uk/MCW/Home.html

[**] We thank the EPSRC and Xunta de Galicia (Angeles Alvariño contract and an Estadías: 2009/188 and 2010/163 to CGR) for support of this work. Additional thanks to Diamond Light Source for beamtime on I19 (MT1858), and Kirsten E. Christensen and David R. Allan for assistance.

Supporting information for this article is available on the WWW under http://dx.doi.org/10.1002/anie.201100956.

Table 1 shows that there is a significant ligand-based *ortho*-substituent effect observed (entries 3–7) for the combination of aldehyde **1a** and phenylacetylene (**2a**). Increasing the size of the *ortho*-substituent results in an increase in the relative amount of the branched isomer produced, with the isopropyl-substituted ligand (**5c**) being most selective, delivering a 3:1 ratio in favor of the branched isomer (Table 1, entry 5). The *t*Bu-substituted ligand did not follow the above trend and resulted in the formation of a considerably less active catalyst (Table 1, entry 7). To confirm the importance of the *ortho*-substituents the corresponding *para*-isopropyl ligand (**5f**) was also evaluated, and in line with use of the parent dppe ligand, delivered the linear isomer as the major product (Table 1, entry 8). This initial ligand analysis demonstrated that for the particular hydroacylation reaction studied, i.e., **1a** + **2a**, it was possible to turn a 1:10 linear-selective system (dppe) into a branched-selective process with a selectivity of 3:1 (**5c**).

With the viability of a ligand-controlled selectivity switch established we next explored the generality of the process. Table 2 documents the reactions between aldehyde **1a** and a range of alkynes, all employing catalysts based on the *i*Pr-substituted ligand **5c**. Both the butyl- and 3-thienyl-substituted alkynes performed similarly to phenylacetylene, delivering the branched isomer as the major product with relatively modest selectivities (Table 2, entries 1 and 2). However, reactions employing electron-deficient arylalkynes were significantly more selective (Table 2, entries 3–6). For example, the use of 4-CF_3-substituted phenylacetylene increased the branched:linear ratio to 8:1 and the corresponding 3,5-di-CF_3-substituted alkyne to >20:1 (Table 2, entries 3 and 4). Non-aromatic alkynes also performed well, with ester- and ketone-substituted examples delivering similarly high selectivities (Table 2, entries 7–9). The final example demonstrates the efficient and selective incorporation of a highly fluorinated alkylalkyne (Table 2, entry 10).

Table 2: Scope of the intermolecular branched-selective hydroacylation employing aldehyde **1a** and substituted alkynes.[a]

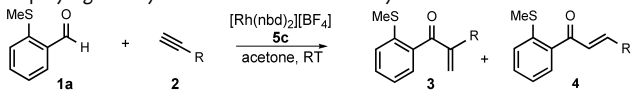

Entry	R	Product	Yield [%][b]	**3**:**4**[c]
1	Bu	**3b**	81	2.5:1
2	3-thienyl	**3c**	79	2.5:1
3	4-CF_3-C_6H_4	**3d**	90	8:1
4	3,5-CF_3-C_6H_3	**3e**	92	>20:1
5	4-NO_2-C_6H_4	**3f**	65	8:1
6	4-CO_2Me-C_6H_4	**3g**	82	4:1
7[d]	CO_2Me	**3h**	63	>20:1
8[d]	CO_2Et	**3i**	82	>20:1
9[d]	COPh	**3j**	53	>20:1
10[d]	$(CF_2)_5CF_3$	**3k**	76	11:1

[a] Conditions: aldehyde **1a** (0.3 mmol), alkyne (0.45 mmol), [Rh(nbd)$_2$][BF$_4$] (10 mol%), ligand **5c** (10 mol%), acetone (2 mL), RT, 2–48 h. [b] Yields of isolated products. [c] Determined by ^{1}H NMR analysis of the crude reaction mixtures. [d] Reactions performed at 50 °C.

Performing the same coupling reactions but employing the catalyst incorporating the parent ligand, dppe, delivers the linear isomers as the major products, but with lower selectivities (e.g. **3d** 1:4.5 branched:linear, **3e** 1:2).

We next explored variation of the aldehyde reaction component; the bis-CF_3-substituted arylalkyne (**2e**), in combination with ligand **5c**, was employed throughout (Table 3).

Table 3: Scope of the intermolecular branched-selective hydroacylation employing alkyne **2e** and varied aldehydes.[a]

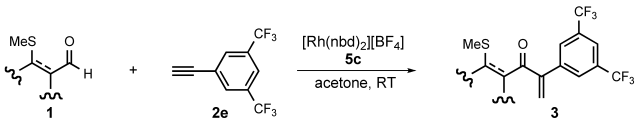

Entry	Aldehyde	Product	Yield [%][b]	**3**:**4**[c]
1	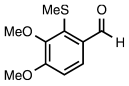	**3l**	83	20:1
2	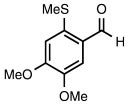	**3m**	93	>20:1
3	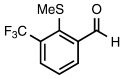	**3n**	82	15:1
4		**3o**	89	>20:1
5[d,e]		**3p**	58	10:1
6[e]		**3q**	75	11:1
7[e]		**3r**	80	13:1
8[e]		**3s**	76	10:1

[a] See Table 2 for conditions. [b] Yields of isolated products. [c] Determined by ^{1}H NMR analysis of the crude reaction mixtures. [d] Substrate used as a 4:1 mixture of diastereomers. [e] Reactions performed at 50 °C.

A variety of aromatic aldehydes featuring both electron-donating and electron-withdrawing substituents delivered the branched enone products with excellent yields and selectivities (Table 3, entries 1–3). The β-*S*-enal employed in entry 4, used for the first time in hydroacylation chemistry, performed equally well, allowing the corresponding bis-enone to be isolated in high yield. The final four entries demonstrate that a range of substituted alkyl aldehydes are also good substrates for the reaction, although a slightly elevated reaction temperatures of 50 °C were required (Table 3, entries 5–8).

To probe the factors behind this switch in selectivity we have studied the structures of the active catalysts in solution and the solid state, as well as closely related model complexes. A suitable pre-catalyst [Rh(**5c**)(acetone)$_2$][BAr$^F_4$] (**6**; Ar^F = $C_6H_3(CF_3)_2$)[10] is formed from hydrogenation of [Rh(**5c**)(nbd)][BAr$^F_4$] in acetone.[11] A solid-state structure of this complex is shown in Figure 1 and confirms a square-planar Rh^I center coordinated with two acetone ligands. The phenyl

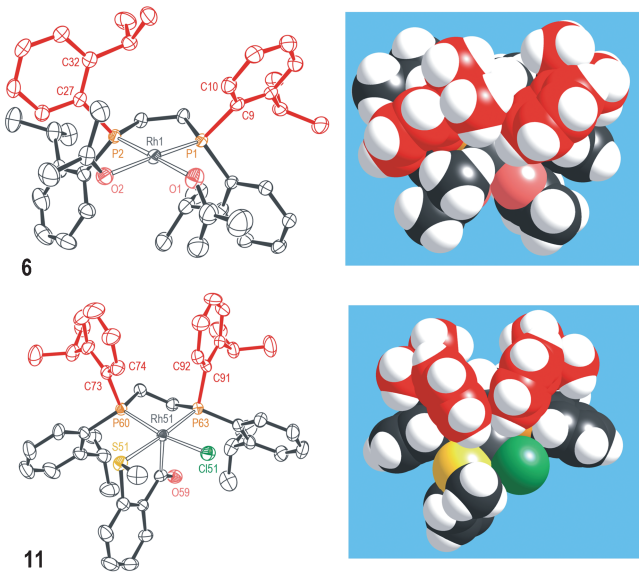

Figure 1. Solid-state structures of **6** and **11**. Thermal ellipsoids at the 50% probability level (left) and Van der Waals radii (right). Phenyl rings for which the dihedral angle has been calculated are highlighted in red. Anion and hydrogen atoms are omitted for clarity.

groups are orientated so that the bulky *i*Pr groups point away from the metal,[9a] although they are still able to adopt a variety of conformations as measured by the dihedral angle of the arenes with respect to the Rh–P bond, for example, Rh1-P2-C27-C32, −74.9(3)°; Rh1-P1-C9-C10, 7.7(3)°.

Addition of aldehyde **1a** to complex **6** results in an equilibrium mixture of Rh^{I} substrate-bound complex [Rh(**5c**){$\kappa^2_{(O,S)}$-(OHC)C_6H_4SMe}][BAr^F_4] (**7**)[12] and the product of oxidative cleavage, [Rh(**5c**)(H){$\kappa^2_{(C,S)}$-(CO)C_6H_4SMe}][BAr^F_4] (**8**; Scheme 2). Complexes **7** and **8** are in exchange with one another at room temperature, and progressive cooling to 200 K resolves separate sharp resonances in the ^{1}H and ^{31}P{^{1}H} NMR spectra. The ratio of **7**:**8** at 200 K is 3:1, which changes to 1:1 at 250 K. At 200 K the spectroscopic markers that identify **7** are a peak centered at $\delta = 10.25$ ppm [d, J(PH) = 6.1 Hz] shifted 0.15 ppm to high frequency from free **1a**, which is assigned to the bound aldehdye; inequivalent

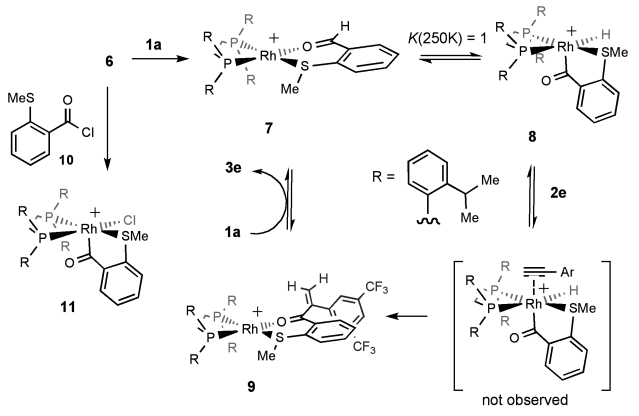

Scheme 2.

^{31}P environments that show coupling to a Rh^{I} center [J(RhP) = 189, 172, J(PP) = 32 Hz]; and separate correlations (^{31}P-^{1}H HMBC) between these and either the aldehdye or the SMe resonances. The Rh^{III} oxidative-addition product, **8**, is characterized at 200 K by a hydride environment that shows coupling to a *trans* phosphine [$\delta = -7.04$ ppm, dd, J(PH) = 169, J(RhH) = 16 Hz], a SMe environment that shows a strong correlation in the ^{31}P/^{1}H-HMBC experiment, and inequivalent phosphorus environments by ^{31}P{^{1}H} NMR spectroscopy, one of which shows a much reduced value for J(RhP) compared with the other (87 versus 160 Hz) identifying it as being opposite the high *trans* influence hydride.[7e] This places the acyl ligand *trans* to the vacant site (or at most, a weakly bound acetone ligand). Similar structures for rhodium acyl hydrides have been noted previously using the DPEphos ligand,[7e] and calculated for the intramolecular hydroacylation of 4-pentenals.[13]

Stoichiometric addition of aldehyde **1a** to **6** followed by one equivalent of alkyne **2e** leads to the spectroscopically characterized product complex [Rh(**5c**){$\kappa^2_{(O,S)}$-$CCH_2(C_6H_3$-$(CF_3)_2)$(OC)C_6H_4SMe}][BAr^F_4] (**9**). Addition of MeCN to **9** liberates branched product **3e** alongside a species characterized as [Rh(**5c**)$(MeCN)_2$][BAr^F_4]; while addition of a further 2 equivalents of aldehyde **1a** to **9** generates a mixture of **7**, **8**, and **9** alongside free product, **3e**, thus demonstrating turnover. Catalysis (10 mol%, 0.02 mol L^{-1} **2e**) is relatively rapid (TOF 60 h^{-1}) and at the end complex **9** is observed. Addition of a further 10 equivalents each of **1a** and **2e** restarted catalysis.

Crystalline material from the mixture of **7** and **8** was not obtained, and to probe in detail the solid-state structures of these intermediates we turned to using the acyl chloride **10**. This underwent clean oxidative addition with **6** to give **11**, [Rh(**5c**)(Cl){$\kappa^2_{(C,S)}$-(OC)C_6H_4SMe}][BAr^F_4], in quantitative yield (by NMR spectroscopy) as a single isomer. A solid-state structure of **11** (as the [BAr^{Cl}_4]$^-$ salt,[14] Figure 1, Ar^{Cl} = 3,5-$Cl_2C_6H_3$) shows an arrangement of ligands exactly as inferred from the spectroscopic characterization of **8** at low temperature, namely a five-coordinate Rh^{III} complex with an acyl group *trans* to a vacant site and the chloride (that is, hydride in **8**) *trans* to a phosphine. Solution NMR data are fully consistent with this description. This structure also gives pointers to the underlying reasons behind the linear/branched selectivity observed in the catalytic process. The oxidative addition of aldehyde to form a Rh^{III} pseudo-octahedral center results in a conformation of the phenyl groups that is far more directional than in precursor **6**, with the arenes pointing directly towards the vacant site on the metal; as shown by the relevant dihedral angles: Rh51-P63-C91-C92, −13.4(5)° and Rh51-P60-C73-C74, 9.7(5)°.

Direct structural comparison between **11** and its dppe analogue would help underscore this idea, as a more flexible orientation of the phenyl groups would correlate with the lower linear/branched selectivities with dppe. Addition of **10** to [Rh(dppe)$(acetone)_2$][BAr^{Cl}_4] gave a product spectroscopically identified as [Rh(dppe)(Cl){$\kappa^2_{(C,S)}$-(OC)C_6H_4SMe}][BAr^{Cl}_4] (**12**), but unfortunately crystals suitable for a X-ray diffraction have proved elusive. However ^{13}C{^{1}H} NMR data for **12** demonstrate free-rotation of the phenyl groups at

293 K, a situation that would not be expected for ligand **5c**.[9b] Restricted rotation in complexes with chelate ligands closely related to **5c** has been noted;[9c] while inspection of the space filling diagram of closely related $[Rh(dppe)(I)_2(COMe)]$[15] (Supporting Information) shows significantly twisted phenyl groups (dihedral −70.8° and −24.7°) compared with **11** suggesting a less rigid conformation for the phenyl groups in dppe. Overall these observations support the idea that the phenyl-group orientation in complex **8**, and in turn the increased selectivity, comes from a minimization of steric strain between the *i*Pr groups and the bound aldehyde at the Rh^{III} center.

That the bulkier product (i.e., branched) is favored with the bulky ligand **5c** suggests that it is the irreversible rate-limiting[16] reductive elimination of the product, for example, **3e**, that controls the final regiochemistry, as the preceding[1a,b,3a,13,16] hydride insertion step would likely favor a linear product when using a bulkier ligand. The progressive increase in selectivity on changing the arene functionalization, H < Me < Et < *i*Pr (Table 1), is consistent with this idea. This scenario requires that the insertion step is fast and reversible.[1b] Reversible insertion of hydrides into alkynes, although rare, has recently been reported on Ir^{III} centers.[17] We have recently suggested a similar scenario in explaining product distributions in competitive alkene versus aldehyde hydroacylation reactions on changing the backbone of a simple chelate ligand;[7h] while faster reductive elimination of branched isomers, and equilbria between linear and branched intermediates, has been noted in $[Cp^*Rh(H_2C{=}CHSiMe_3)_2]$ ($Cp^* = \eta^5$-C_5Me_5) catalyst systems.[1b] The experimental observation that electron-poor alkynes give the best selectivities could, in part, also be related to an enhanced rate of reductive elimination associated with these alkynes.[1b]

Scheme 3 demonstrates the utility of our developed methodology. The first two reactions illustrate the switch in regioselectivity now achievable by the correct choice of ligand; the combination of aldehyde **1q** and alkyne **2e** using the *ortho*-*i*Pr-dppe-derived catalyst selectively delivers the branched adduct (**3q**, 1:11 linear/branched). Employing the catalyst incorporating dppe delivers the linear isomer as the major product with 2:1 selectivity. However, use of a DPEphos-derived catalyst[7d,e] leads to efficient formation of the linear isomer with 20:1 selectivity. The third transformation illustrates the utility of the *exo*-methylene products in a simple application to a one-pot three-component coupling; rather than isolate the branched adduct obtained from the union of aldehyde **1a** and alkyne **2e**, reaction with indole in 1,2-dichloroethane (DCE) at 80 °C results in direct conjugate addition and allows substituted ketone **13** (see the Supporting Information) to be isolated in 88% yield.

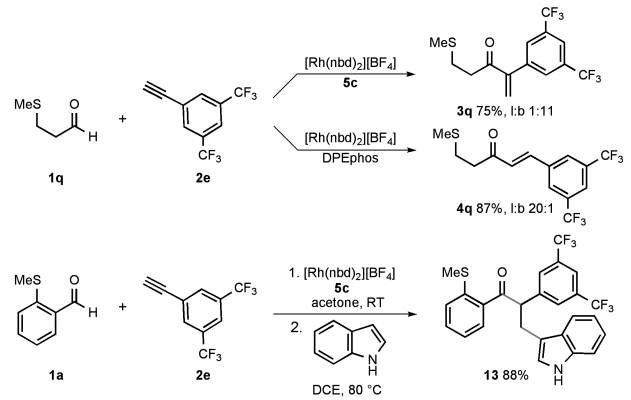

Scheme 3.

In conclusion, we have developed a system that provides control over regioselectivity in the hydroacylation of alkynes, especially electron-poor derivatives, in which a bulky *ortho*-*i*Pr-dppe-derived catalyst promotes the formation of the branched adduct. In this regard these results contrast to the closely related alkene hydroformylation, in which bulky ligands promote linear products.[18] This may be related to the suggested rate-limiting step in each: reductive elimination in olefin hydroacylation and hydride insertion in hydroformylation. Future contributions will explore and exploit the mechanism in more detail.

Received: February 7, 2011
Published online: April 19, 2011

Keywords: alkynes · hydroacylation · regioselectivity · rhodium catalysis

[1] Recent examples: a) Y.-T. Hong, A. Barchuk, M. J. Krische, *Angew. Chem.* **2006**, *118*, 7039; *Angew. Chem. Int. Ed.* **2006**, *45*, 6885; b) A. H. Roy, C. P. Lenges, M. Brookhart, *J. Am. Chem. Soc.* **2007**, *129*, 2082; c) S. Omura, T. Fukuyama, J. Horiguchi, Y. Murakami, I. Ryu, *J. Am. Chem. Soc.* **2008**, *130*, 14094; d) F. Shibahara, J. F. Bower, M. J. Krische, *J. Am. Chem. Soc.* **2008**, *130*, 14120; e) V. M. Williams, J. C. Leung, R. L. Patman, M. J. Krische, *Tetrahedron* **2009**, *65*, 5024.

[2] Recent examples: a) M. Imai, M. Tanaka, K. Tanaka, Y. Yamamoto, N. Imai-Ogata, M. Shimowatari, S. Nagumo, N. Kawahara, H. Suemune, *J. Org. Chem.* **2004**, *69*, 1144; b) T. Tanaka, M. Tanaka, H. Suemune, *Tetrahedron Lett.* **2005**, *46*, 6053; c) K. Tanaka, Y. Shibata, T. Suda, Y. Hagiwara, M. Hirano, *Org. Lett.* **2007**, *9*, 1215.

[3] a) M. C. Willis, *Chem. Rev.* **2010**, *110*, 725; b) C.-H. Jun, E.-A. Jo, J.-W. Park, *Eur. J. Org. Chem.* **2007**, 1869.

[4] a) R. T. Stemmler, C. Bolm, *Adv. Synth. Catal.* **2007**, *349*, 1185; b) J. D. Osborne, H. E Randell-Sly, G. S. Currie, A. R. Cowley, M. C. Willis, *J. Am. Chem. Soc.* **2008**, *130*, 17232; c) Y. Shibata, K. Tanaka, *J. Am. Chem. Soc.* **2009**, *131*, 12552; d) Y. Inui, M. Tanaka, M. Imai, K. Tanaka, H. Suemune, *Chem. Pharm. Bull.* **2009**, *57*, 1158; e) C. González-Rodríguez, S. R. Parsons, A. L. Thompson, M. C. Willis, *Chem. Eur. J.* **2010**, *16*, 10950; f) D. T. H. Phan, K. G. M. Kou, V. M. Dong, *J. Am. Chem. Soc.* **2010**, *132*, 16354; g) M. C. Coulter, K. G. M. Kou, B. Galligan, V. M. Dong, *J. Am. Chem. Soc.* **2010**, *132*, 16330.

[5] C-H. Jun, H. Lee, J.-B. Hong, B.-I. Kwon, *Angew. Chem.* **2002**, *114*, 2250; *Angew. Chem. Int. Ed.* **2002**, *41*, 2146.

[6] Dong et al. have described a ligand-controlled branched to linear switch for a single substrate employed in an intramolecular Rh-catalyzed alkene hydroacylation: M. M. Coulter, P. K. Dornan, V. M. Dong, *J. Am. Chem. Soc.* **2009**, *131*, 6932.

[7] a) M. C. Willis, S. J. McNally, P. J. Beswick, *Angew. Chem.* **2004**, *116*, 344; *Angew. Chem. Int. Ed.* **2004**, *43*, 340; b) M. C. Willis, H. E. Randell-Sly, R. L. Woodward, G. S. Currie, *Org. Lett.* **2005**, *7*, 2249; c) M. C. Willis, H. E. Randell-Sly, R. L. Woodward, S. J. McNally, G. S. Currie, *J. Org. Chem.* **2006**, *71*, 5291; d) G. L. Moxham, H. E. Randell-Sly, S. K. Brayshaw, R. L. Woodward,

A. S. Weller, M. C. Willis, *Angew. Chem.* **2006**, *118*, 7780; *Angew. Chem. Int. Ed.* **2006**, *45*, 7618; e) G. L. Moxham, H. E. Randell-Sly, S. K. Brayshaw, A. S. Weller, M. C. Willis, *Chem. Eur. J.* **2008**, *14*, 8383; f) J. D. Osborne, M. C. Willis, *Chem. Commun.* **2008**, 5025; g) H. E. Randell-Sly, J. D. Osborne, R. L. Woodward, G. S. Currie, M. C. Willis, *Tetrahedron* **2009**, *65*, 5110; h) R. J. Pawley, G. L. Moxham, R. Dallanegra, A. B. Chaplin, S. K. Brayshaw, A. S. Weller, M. C. Willis, *Organometallics* **2010**, *29*, 1717.

[8] Specific substrate combinations lead to branched products: vinylsulfone,[7a] diene,[7a] nitrile-substituted alkyne.[7c]

[9] a) J. N. L. Dennett. A. L. Gillon, K. Heslop, D. J. Hyett, J. S. Fleming, C. E. Lloyd-Jones, A. G. Orpen, P. G. Pringle, D. F. Wass, J. N. Scutt, R. H. Weatherhead, *Organometallics* **2004**, *23*, 6077; b) R. A. Baber, A. G. Orpen, P. G. Pringle, M. J. Wilkinson, R. L. Wingad, *Dalton Trans.* **2005**, 659; c) S. J. Dossett, A. Gillon, A. G. Orpen, J. S. Fleming, P. G. Pringle, D. F. Wass, M. D. Jones, *Chem. Commun.* **2001**, 699.

[10] We find no significant difference in selectivity with the use of $[BF_4]^-$ and $[BAr^F_4]^-$ anions for the conditions reported in Tables 1 and 2.

[11] Crystallographic data. **6**: $C_{76}H_{72}BF_{24}O_2P_2Rh$, $M = 1649.00$, monoclinic, $P2_1/n$ ($Z = 4$), $a = 19.8241(2)$ Å, $b = 20.2882(2)$ Å, $c = 21.4016(2)$ Å, $\beta = 111.5098(4)°$. $V = 1043.25(7)$ Å^3, $T = 150(2)$ K, 16254 unique reflections [R(int) = 0.0255]. Final $R_1 = 0.0510$ [$I > 2\sigma(I)$]. **11**·0.89 acetone: $C_{72.66}H_{72.31}BCl_9O_{1.89}P_2RhS$, $M = 1502.52$, triclinic, $P\bar{1}$ ($Z = 4$, $Z' = 2$), $a = 12.8020(16)$ Å, $b = 18.794(2)$ Å, $c = 31.915(4)$ Å, $\alpha = 99.370(2)°$, $\beta = 93.1700(10)°$, $\gamma = 104.344(2)°$. $V = 7303.3(16)$ Å^3, $T = 150(2)$ K, 23810 unique reflections [R(int) = 0.112]. Final $R_1 = 0.0621$ [$I > 2\sigma(I)$]. CCDC 804185 (**6**), CCDC 804186 (**11**), and CCDC 815141 (**13**) contain the supplementary crystallographic data for this paper. These data can be obtained free of charge from The Cambridge Crystallographic Data Centre via www.ccdc.cam.ac.uk/data_request/cif.

[12] Complex **7** is formed as an approximate 1:0.37 mixture of two isomers, see Figure S-1 (Supporting Information). Both show correlations between CHO and SMe to different phosphines in the $^{31}P\{^1H\}$ NMR spectrum and appear as broad doublets (CHO) in the ^1H NMR spectrum at 200 K. Both complexes are consumed on addition of alkyne **2e**. We suggest that these isomers are due to restricted rotation of the bulky arene groups and/or restricted inversion at sulfur.

[13] I. F. D. Hyatt, H. K. Anderson, A. T. Morehead, A. L. Sargent, *Organometallics* **2008**, *27*, 135.

[14] A. B. Chaplin, A. S. Weller, *Eur. J. Inorg. Chem.* **2010**, 5124.

[15] L. Gonsalvi, H. Adams, G. J. Sunley, E. Ditzel, A. Haynes, *J. Am. Chem. Soc.* **2002**, *124*, 13597.

[16] D. P. Fairlie, B. Bosnich, *Organometallics* **1988**, *7*, 946.

[17] R. Ghosh, X. Zhang, P. Achord, T. J. Emge, K. Krogh-Jespersen, A. S. Goldman, *J. Am. Chem. Soc.* **2007**, *129*, 853.

[18] Z. Freixa, P. W. N. M. van Leeuwen, *Dalton Trans.* **2003**, 1890.

